EEET ECOLOGICAL ENGINEERING
& ENVIRONMENTAL TECHNOLOGY

Ecological Engineering & Environmental Technology 2024, 25(10), 87–95
https://doi.org/10.12912/27197050/191332
ISSN 2299–8993, License CC-BY 4.0

Received: 2024.07.03
Accepted: 2024.08.15
Published: 2024.09.01

Relationships Among Global Climate Indices, Rainfall Patterns, and Crop Productivity in the Southern Part of Java, Indonesia

Bayu Dwi Apri Nugroho[1*], Chusnul Arif[2], Fadila Suryandika[3], Hertiyana Nur Annisa[1], Syintianuri Intan Wijayanti[4]

[1] Department of Agricultural and Biosystem Engineering, Universitas Gadjah Mada, Yogyakarta, Indonesia
[2] Department of Civil and Environmental Engineering, IPB University, Bogor, West Java, Indonesia
[3] Department of Agricultural, Universitas Pembangunan Nasional Veteran Jawa Timur, East Java, Indonesia
[4] Department of Soil Science, Universitas Gadjah Mada, Yogyakarta, Indonesia
* Corresponding author's e-mail: bayu.tep@ugm.ac.id

ABSTRACT

In tropical countries, especially Indonesia, even though there is a notable correlation between rainfall pattern and indices of global climate, limited proof exists regarding the impact on crop productivity. Global climate indices are one of the indicators to identify the occurrence of climate change, but there is little research on climate change in Indonesia. In this research, the relationships among indices of global climate are represented by the southern oscillation index (SOI) and the sea surface temperature (SST) such as Nino. West, the Indian Ocean Basin-Wide (IOBW), and Nino 3, then the pattern of rainfall distribution and crop productivity during 10 years from 2012 to 2022 in the southern part of Java. The southern part of Java which is represented by Gunung Kidul District is a rain-fed area, and its location is in hilly topography so rainfall will be an important factor in this area, not only for daily life but also for agricultural sector purposes. The purpose of the study was to discover the relationship between global climate indices, rainfall distribution pattern and crop productivity in the Southern Part of Java, Indonesia. Rainfall distribution pattern for 10 years was calculated and displayed with spatial method, then principal component analysis (PCA) was used to analyse SST, and correlation analyses were used, along with wet and dry seasons as well as crop productivity. The results showed that from 2012 to 2022, high rainfall and correlation with global climate indices occurred in the southern and western part of Gunung Kidul district, and correlation among rainfall patterns and crop productivity showed significant correlations in some sub-districts. This result also showed that the relationships among global climate indices and rainfall distribution pattern can be influenced the agricultural productivity in the rainfed areas.

Keywords: climate variability, rainfed agriculture, agricultural productivity, principal component analysis.

INTRODUCTION

In rain-fed agriculture, the occurrence of El Niño tends to delay the start of the wet season, which usually lasts from October to March, thereby negatively impacting agricultural production (Ubilava, 2019). Over the last two decades, multiple El Niño events (McPhaden, 1999) have led to delays in paddy harvesting across Indonesia, posing a threat to food availability (Amien et al., 1996; Harger, 1995). The agricultural decline experienced in Indonesia during the 1997/1998 and 1982/1983 periods had significant economic repercussions, causing an estimated loss of approximately US$2.75 billion. This contributed substantially to the country's overall losses, which totalled nearly US$9 billion (Kirono and Tapper, 1999). Specifically on the island of Java, certain highland sub-districts experienced a significant drop in rain-fed paddy yields. In these areas, particularly in the southern highland regions, dryland yields decreased dramatically by 52% (Vindari, 2022). This decline was primarily attributed to the delayed onset of the rainy season. Therefore, it becomes crucial to conduct thorough investigations into the relationship between variability in wet season rainfall and the yields of rain-fed crops in mountain topography.

Some studies have delved into the connection in Indonesia between variations in precipitation and the highland areas. Shetty (2022) demonstrated that the windward regions of the highlands in western Sumatra experience higher levels of precipitation and wind speed, compared to the leeward side. This suggests that surface topography influences not only rainfall distribution in Sumatra but also across the wider Indonesian archipelago.

Restitiasih et al., (2019) discovered a correlation between rainfall variations in Indonesia and global climate indicators, such as the SOI and SST. Significant SST variations occur notably in Indonesia, and the adjacent tropical Pacific area (Trenberth and Shea, 1987; Trenberth and Hoar, 1996). Nicholls (1984) highlighted the effectiveness of surface pressure recordings in Darwin, northern Australia, along with SST levels surrounding Indonesia, in predicting climate changes and rainfall trends within the Indonesian region. Moreover, Kirono and Tapper (1999) identified a direct link between rainfall patterns from June to November, as well as SOI observed between 1951 and 1997. This correlation was strong in the southern part of Java, notably within the Gunung Kidul District.

Consequently, rain-fed crop cultivation in Indonesia's highland regions is shaped by multiple factors, encompassing rainfall variations, global climate indicators like the Nino3, Nino.West indices, and the distinctive topography characterizing these highland areas (Li et al., 2019). Hence, this study aims to elucidate the connections between indices of global climate (specifically the SOI and SSTs), precipitation distribution patterns, and productivity of crops spanning years from 2012 to 2022. By establishing these relationships, this research can provided predict agricultural yields and develop strategies to mitigate the adverse effects of climate variability on rain-fed agriculture in this region.

MATERIALS AND METHODS

Research area

The conducted research is concentrated in the Southern Part of Java, which is centered on Gunung Kidul District, situated between 7°46'–7°09'S and 110°21'–110°50'E, characterized by rainfed agriculture land in the elevated terrains of the Southern Part of Java, bordering with the Indian Ocean. Encompassing an area of 1485.36 km^2, this region consists into 18 sub-districts, and 144 villages (Gunung Kidulkab, 2023). About 61.989 hectares of agricultural land in this area rely on rain-fed practices, with a specific focus on the importance of October precipitation (Gunung Kidul Agricultural Office, 2023), while 7.804 hectares are under irrigation. The average annual precipitation recorded in the district between 2013 and 2016 stood at 2041 mm. Both the wet and dry seasons typically extend for 5 to 6 months each (Gunung Kidul Agricultural Office, 2023).

Primary crops cultivated here include dryland paddy and various other dryland food crops, such as corn, cassava, and soybean. There are two primary cropping systems: monoculture and multiple cropping (Ding et al., 2024).

Monoculture involves cultivating the same crop repeatedly on specific land, often seen in wetland or irrigated regions (Bockstaller et al., 2024). On the other hand, multiple cropping involves growing two, three or more crops successively on the same area within a scheduled year (Huang, 2003; Beets, 1975), commonly practiced in rainfed agricultural fields (Sarjiman and Mulyadi, 2005).

In the elevated rainfed terrains of Gunung Kidul district, intercropping is the primary cultivation method. Cassava dominates crop production, accounting for approximately 62% of the total output. Other significant crops include dryland paddy (11.4%), soybean (5.5%), peanut (8%), maize (9.6%), and wetland paddy rice (3.3%) (Gunung Kidul Agricultural Office, 2023). The prominence of Cassava in the multiple cropping system of the district is due to its year-round growth potential and resilience against drought conditions (Gunung Kidul Agricultural Office, 2023).

Data

Crop productivity

Between 2012 and 2022, annual crop productivity information for dryland paddy, corn, cassava, and soybean was collected from twelve subdistricts within Gunung Kidul: Rongkop, Tepus, Paliyan, Panggang, Semanu, Patuk, Nglipar, Gedangsari, Ponjong, Karangmojo, Wonosari and Playen (Fig. 1). Unfortunately, data from six sub-districts such as Girisubo, Gedangsari, Tanjungsari, Semin, Saptosari and Ngawen could not be included in this analysis due to insufficient

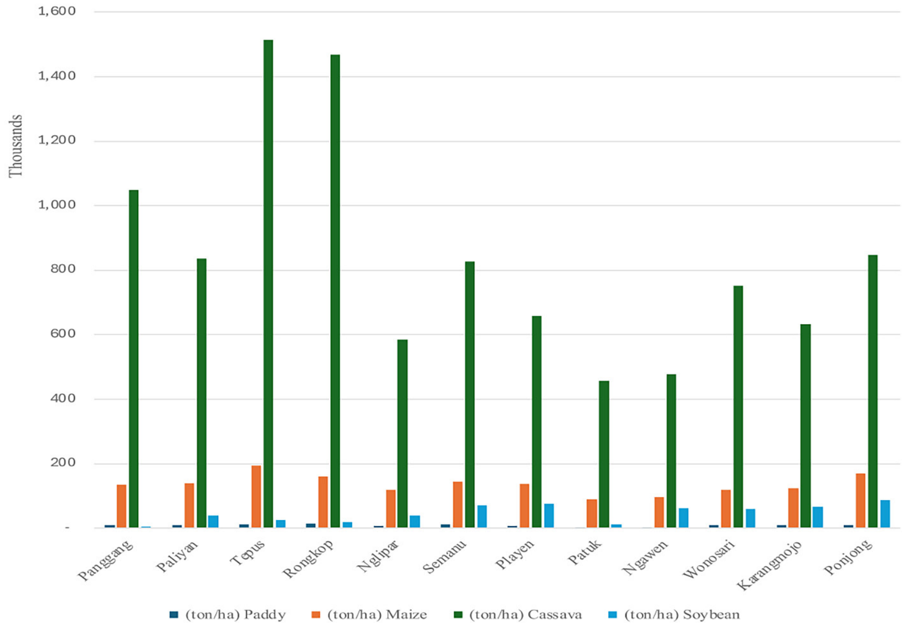

Figure 1. Average productivity of each crop in all sub districts from 2012 to 2022 in Gunung Kidul District

available data. For the analysis, crop yield residuals were calculated according to the method described by Martinez et al. (2009) as follows:

$$y_{residual} = \frac{y_{observed}}{y_{smoothed}} - 1 \quad (1)$$

To avoid reliability issues and errors associated with the data, such as human error when submitted data, a low-pass spectral smoothing filter with a 5-year moving average (Press et al., 1989) was used to detrend the observed crop yields. Each data was regularized (mean = 0) to allow for the direct observation of statistical fluctuations in agricultural yields for each sub-district, while the residuals preserved the trend of each data.

Rainfall data

From 2012 to 2022, rainfall data was collected from twelve stations (Gunung Kidul Agricultural Office, 2023). Specifically, the data from twelve out of the eighteen stations of rainfall observation, selected based on the availability of sufficient data, were utilized. Subsequently, three distribution pattern analyses were conducted: one spanning six months (October to March), another focusing on October-November-December (OND), and the third examining January-February-March (JFM). The JFM and OND analyses were undertaken to represent the beginning and peak of the wet season, respectively (Fig. 2). Following this,

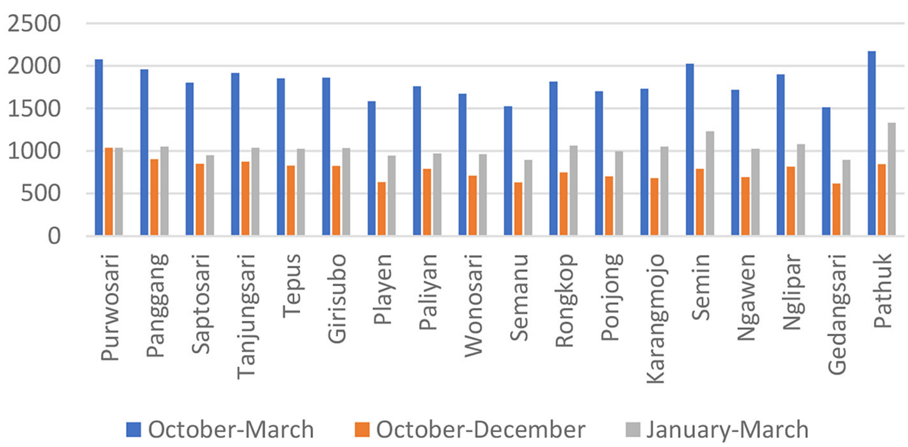

Figure 2. Rainfall data in all sub district from 2012 to 2022 in Gunung Kidul District

the average seasonal rainfall values for normal years were analysed using a Monte Carlo Bootstrap resampling process with 1000 samples. This involves generating a bootstrap sample, denoted as X^*, by resampling the initial data set X, which has a size of n, with replacement, repeating this process n times (n = 1000), where X represents the initial sample data to be analysed, such as neutral year rainfall data, and n is the number of data points to be resampled (1000).

$$X^* = (X_1^*, X_2^*, X_3^*, \dots, X_n^*) \quad (2)$$

Subsequently, statistical calculations were performed for each bootstrap sample. A statistical function T was applied to each bootstrap sample, resulting in a value denoted as T^*.

$$T^* = T\ (X^*) \quad (3)$$

Indices of global climate (southern oscillation index and sea surface temperature)

From 2012 to 2022, data pertaining to SOI and SSTs were employed as representations of global climate indices in this investigation. Monthly SOI and averaged SSTs within distinct regions – Niño. West (15°N–0°, 130°E–150°E), Indian Ocean Basin Wide (IOBW; 20°N–20°S, 40°E–100°E), and Niño 3.4 (5°N–5°S, 120°E–170°E) were obtained from NASA (Fig. 3).

Initially, to align with the analysis objectives, it was necessary to recalculate the values of SOI and SST by averaging over 2-month periods OND and JFM, with a 6-month interval covering each wet season in the months (October, November, December, January, February, March). Subsequently, the SST data from the Niño 3.4, Niño. West, and IOBW regions were integrated using principal component analysis (PCA). The aim was to provide a direct comparison between rainfall data and SST. In this specific study, only the main principal component (PC) that has contributed a minimum of 70% of the cumulative variance proportion was used in correlation analysis, along with other datasets (Bayu et al., 2013).

RESULTS AND DISCUSSIONS

Principal components (PC) for the SSTs

Table 1 displays the PC and their corresponding statistical variances. Notably, the first PC (PC1) of the IOBW and Niño.3 regions exhibits

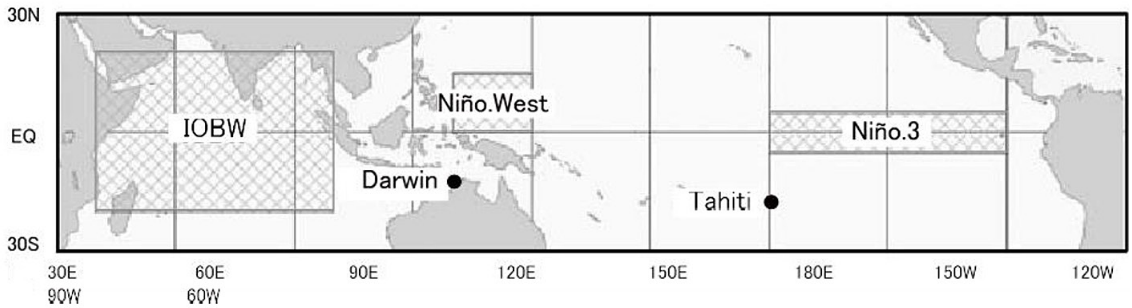

Figure 3. The three El Niño monitoring regions (shaded areas) are used to observe the relationship among sea surface temperatures in the eastern Pacific (Niño 3), the western Pacific (Niño West), and the Indian Ocean (IOBW)

Table 1. PC loadings and their importance of components for each PC against the SSTs (Niño. 3, Niño. West and IOBW)

Parameter	PC1	PC2	PC3
Regions of SST			
IOBW	0.53	0.70	-0.48
Nino West	-0.53	0.72	0.46
Nino 3	0.67	0.01	0.75
Importance of components			
Standart deviation	1.49	0.86	0.24
Proportion of variance	0.74	0.25	0.02
Cumulative proportion	0.74	0.98	1.00

positive loadings, indicating a synchronous nature in the sea surface temperatures (SSTs) observed within these two areas (Zhang, 2021). In contrast, PC1 is highly linked to El Niño and/or La Niña episodes, as seen by the comparison of Niño.3 and Niño. West. Because PC1 accounted for more than 70% of the variation overall, it was the only model used to describe the SSTs for the three areas for the purposes of this study (Fig. 4).

Rainfall distribution pattern

In the conducted analysis of rainfall patterns covering the years 2012 to 2022, the data for six months of the wet season were considered, with a specific emphasis on the periods of October to November to December and January to February to March (Fig. 5). Throughout the entirety of the wet season, the western inland and southern coastal regions witnessed rainfall fluctuations ranging between 1800 and 2200 mm, while the northern and lowland areas received approximately 1700–1850 mm of rainfall (Fig. 5a).

In the initial phase of the wet season (OND), rainfall ranged from 850 to 1050 mm in the southern coastal areas and 650 to 750 mm in the central lowlands (Fig. 5b). However, the most substantial rainfall was observed during the latter part of the wet season (JFM, Fig. 5c). Specifically, during the height of the rainy season in January, moisture originating from the Indian Ocean is conveyed to Java through westerly winds (Hermawan, 2022). The air, saturated with moisture and driven by the winds, gives rise to thick clouds and orographic precipitation (Roe, 2005) in the mountainous areas of southern and western Java.

Association of SSTs and rainfall

In this research, a mapping analysis was conducted to explore the relationships between indices of global climate (specifically PCI and SSO SST) and rainfall patterns from 2012 to 2022 in Gunung Kidul district. Figure 3 illustrates that nearly all sub-districts within Gunung Kidul exhibit noteworthy correlations between indices of global climate and precipitation. Comparisons were conducted between average rainfall for the period of 2012 to 2022 and PC1 of SSTs in three distinct analyses: spanning October to March, representing the area's six-month rainy season; OND, or October-November-December, denoting the season's beginning; and JFM, or January-February-March, denoting its conclusion. All of the sub-districts in the Gunung Kidul District showed substantial relationships between PC1 SSTs and average precipitation in OND, according to the conducted research. Table 2 presents comprehensive findings.

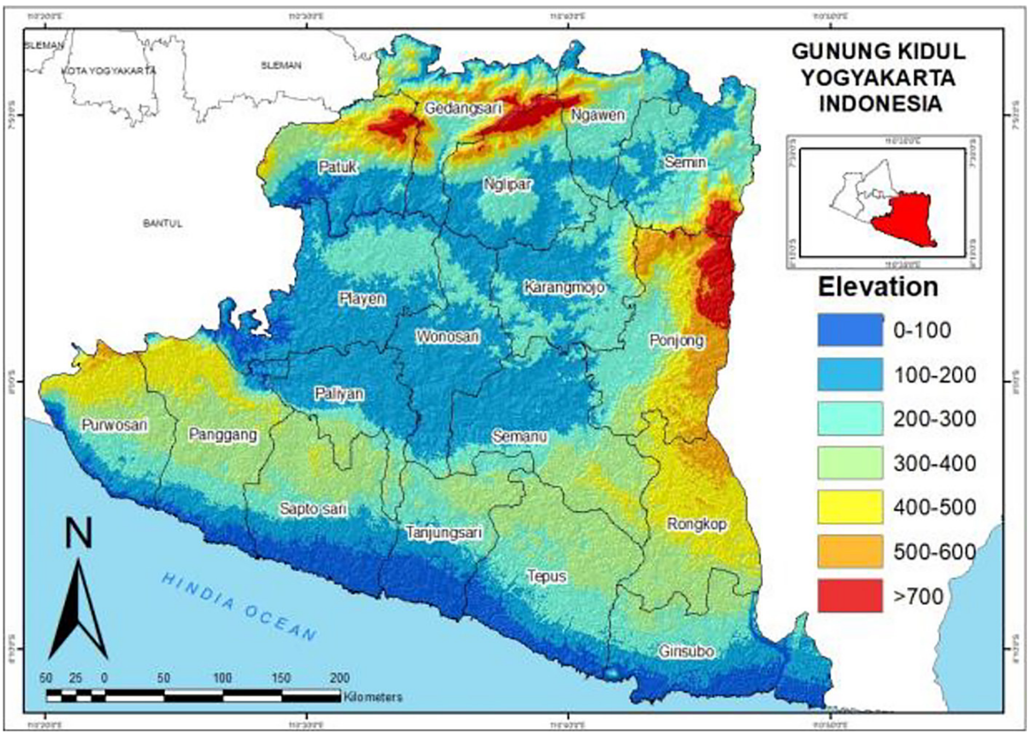

Figure 4. Study area and topography in 18 sub-districts.

a)

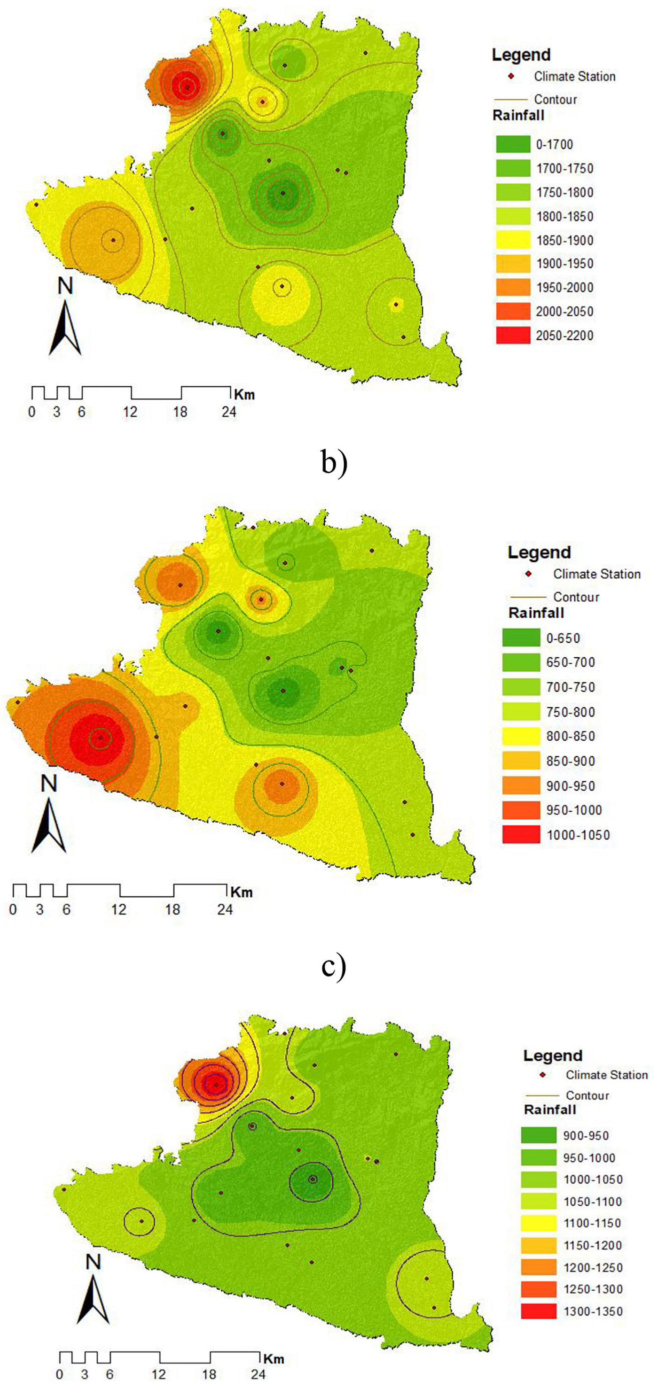

Figure 5 a) Pattern of rainfall distribution during the wet season (October, November, December, January, and March) from 2012 to 2022; b) Pattern of rainfall distribution during the period October-November-December (OND) from 2012 to 2022; c) Pattern of rainfall distribution during the period January-February-March (JFM) from 2012 to 2022

Association between indices of global climate and crops productivity

Figure 6 shows the relationships between indices of global climate with crop productivity in Gunung Kidul district from 2012 to 2022. Figure 7 shows a pattern of correlations, in the west of Gunung Kidul district, with some sub-districts having significant correlations between indices of global climate with crop productivity (dryland

Tabel 2. Pearson's correlation between the PC1 and rainfall (OND and JFM) for each district of the study area

District	Rainfall	
	JFM	OND
Karangmojo	0.01	-0.52*
Ngawen	0.19	-0.31
Nglipar	0.47	-0.56**
Paliyan	-0.38	-0.41**
Panggang	-0.32	-0.54*
Patuk	0.17	-0.074
Playen	-0.11	-0.63**
Ponjong	-0.37	0.509*
Rongkop	-0.03	-0.64**
Semanu	0.07	0.56*
Tepus	0.13	-0.43*
Wonosari	0.17	-0.65**

paddy, cassava, corn, and soybean). There is a correlation between crop productivity in the eastern Gunung Kidul district and global climate indices, namely SOI and PC1 SST (Maharani, 2023). Detail of correlations between indices of global climate with crop productivity (dryland paddy, soybean, corn and cassava) Table 3. Table 3 shows that almost all sub-districts have a significant relationship between indices of global climate with crop productivity (dry land paddy, cassava, corn, and soybean).

PC1 SSTs have positive correlations, and SOI shows negative correlations with crop productivity (Fig. 7). This observation suggests that certain sub-districts had correlations with global climate indices in relation to crops like soybean, corn, and paddy (Zhou, 2021).

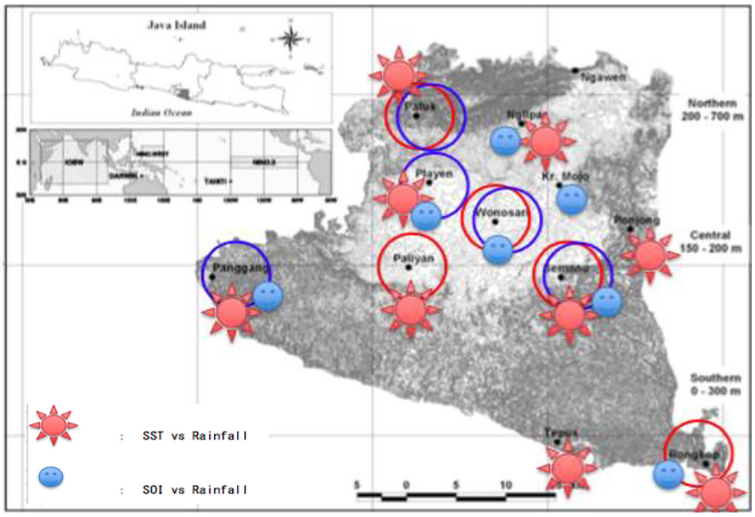

Figure 6. Significant relationship among rainfall - PCI SST and SOI for each sub-district

Table 3. The crop production (dry paddy, corn, cassava, and soybean) in the districts of the study area and the global climatic indices (SOI and PC1) were correlated by Pearson

District	SOI vs Crop residuals				PC1 vs Crop residuals			
	Dry	Cassava	Corn	Soybean	Dry	Cassava	Corn	Soybean
Karang Mojo	0.19	0.09	-0.02	0.31	-0.11	-0.01	0.06	-0.36
Ngawen	0.15	-0.14	-0.20	0.23	0.01	0.11	0.02	-0.22
Nglipar	0.36	-0.23	-0.13	-0.06	-0.32	0.28	0.03	0.07
Paliyan	0.22	0.29	0.13	0.33	-0.26	-0.31	-0.20	-0.40
Panggang	0.51*	-0.15	0.44	0.39	-0.43	0.42	-0.37	-0.31
Patuk	0.53*	0.08	0.37	0.43	-0.42	-0.02	-0.34	-0.51*
Playen	0.41	-0.33	-0.18	0.42	-0.41	0.46	0.20	-0.31
Ponjong	0.27	-0.12	0.30	0.20	-0.28	0.23	-0.22	-0.41
Rongkop	0.09	0.21	0.32	0.49	-0.16	-0.03	-0.29	-0.51*
Semanu	-0.08	-0.23	0.31	0.49	0.12	0.34	-0.39	-0.61*
Tepus	-0.13	-0.23	0.22	0.35	0.31	0.31	-0.19	-0.36
Wonosari	0.21	-0.19	0.50*	0.23	-0.15	0.27	-0.52*	-0.42

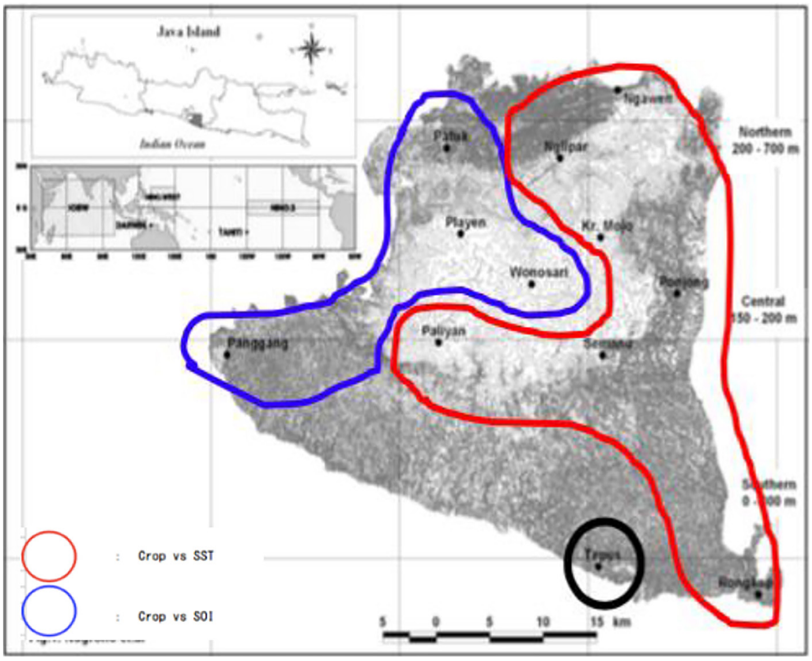

Figure 7. Correlation between global climate indices (PC1 SST with red colour and SOI with blue colour) with crop productivity (dryland, corn, paddy, soybean and cassava) in the study area

CONCLUSIONS

This research explored correlation between indices of global climate and the precipitation patterns observed in the elevated regions of the Southern part of Java, Indonesia. The investigation involves summarizing sea surface temperatures using principal component analysis and determining the residuals in rainfall data for individual stations within the specified research area. The observed trend of rainfall distribution highlighted that from 2012 to 2022, during the rainy season, a majority of rainfall occurred in the mountainous regions to the south and west, especially along the coastline.

Conversely, the central lowland areas received comparatively less rainfall. Within these lowlands, characterized by hilly terrain, variations in rainfall amounts among sub-districts were influenced by prevailing wind directions and orographic effects. Most subdistricts displayed a significant relationship between rainfall and PC1 SSTs during October-November-December. Additionally, global climate indices exhibited correlations with average rainfall across nearly all subdistricts. Notably, PC1 SSTs displayed a significant correlation with crop productivity in the eastern region while the SOI showed a significant correlation in the western part of Gunung Kidul district.

Acknowledgements

This research is supported by Research Center of Land Resources Development, Universitas Gadjah Mada, Yogyakarta, Indonesia.

REFERENCES

1. Agricultural Service for Food Crops and Horticulture, Gunung Kidul district. 2009. Rainfall database in GunungKidul district, 10–130.
2. Anders, A.M., Roe, G.H., Hallet, B., Montgomery D.R., Finnegan, N.J., Putkonen J. 2006. Spatial patterns of precipitation and topography in the Himalaya. Geological Society of America 398, 39–53.
3. Bayu, D.A.N., Ardiansyah, O.D.P., Kanno, H., Sameshima, R., Fujii, H., Lopez, L.C.M.. 2013. Relationships between global climate indices and rain-fed crop yields in highland of South-Central Java, Indonesia, Journal of Geography 122 (3), 438–447.
4. Gunung Kidul Agricultural Office, Gunung Kidul district. 2023. Rainfall database in Gunung Kidul district, 10–130.
5. Gunungkidul district, Indonesia. 2016. Geographical conditions in GunungKidul district. http://www.gunungkidulkab.go.id/home.php?mode=content&id=78
6. Hamada J.I., Yamanaka M.D., Mori S., Tauhid Y.I., Sribimawati. 2008. Differences of rainfall characteristics between coastal and inferior areas of central

western Sumatera, Indonesia. Journal of the Meteorological Society of Japan, 86(5), 593–611.

7. Haylock, M., McBride J. 2001 Spatial coherence and predictability of Indonesian wet season rainfall. J. Climate 14, 3882–3887.
8. Japan Meteorological Agency, 2010. El Nino Index data, retrieved from the statistical climate service at http://www.data.jma.go.jp/gmd/cpd/db/elnino/index/dattab.html
9. Kirono D.G.C and Tapper N.J. 1999. ENSO rainfall variability and impacts on crop production in Indonesia. Physical Geography, 20, 6, 508–519.
10. Maharani, D., Sudomo, A., Swestiani, D., Handayani, W. 2023. Land optimization using tubers based agroforestry system in Semin, Gunung Kidul. IOP Conference Series: Earth and Environmental Science, 1160. https://doi.org/10.1088/1755-1315/1160/1/012069
11. Martinez, C.J., Baigorria, G.A. and Jones, J.W. 2009. Use of climate indices to predict corn yields in southeast USA. International Journal of Climatology, 29, 1680–1691.
12. Massari, C., Brocca, L., Pellarin, T., Abramowitz, G., Filippucci, P., Ciabatta, L., Maggioni, V., Kerr, Y., Prieto, D. 2020. A daily 25 km short-latency rainfall product for data-scarce regions based on the integration of the Global Precipitation Measurement mission rainfall and multiple-satellite soil moisture products. Hydrology and Earth System Sciences. https://doi.org/10.5194/hess-24-2687-2020
13. Ngongo, Y., Basuki, T., deRosari, B., Mau, Y., Noerwijati, K., daSilva, H., Sitorus, A., Kotta, N., Utomo, W., Wisnubroto, E. 2022. The roles of cassava in marginal semi-arid farming in East Nusa Tenggara—Indonesia. Sustainability. https://doi.org/10.3390/su14095439
14. Nicholls N. 1981. Air-sea interaction and the possibility of long-range weather prediction in the Indonesian archipelago. Mon. Wea. Rev., 109, 2435–2443.
15. Nicholls N. 1984. The Southern Oscillation and Indonesia sea surface temperature. Mon. Wea. Rev., 112, 424–432.
16. Yamazaki, N., Kamahori, H., Takahashi, K., Kadokura, S., Wada, K., Kato, K., Oyama, R., Ose, T., Mannoji N., Taira, R. 2007. The JRA-25 Reanalysis. J. Meteor. Soc. Japan, 85, 369–432.
17. Press, W.H., Flannery, B.P., Teukolsky, S.A. and Vet- terling, W.T. 1989. Numerical Recipes: The Art of Scientific Computing. Cambridge University Press, New York, NY, USA, 702.
18. Restitiasih, W.M., Sukarasa, I.K., Yuda, I.W.A., 2019. The Correlation of Southern Oscillation Index (SOI) with the Rainfall at Rainy and Dry Season Peak in Kintamani-Bangli Region period 1986–2015. Buletin Fisika, 20, 6–11.
19. Roe, G.H. 2005 Orographic precipitation. Annu. Rev. Earth Planet. Sci 33, 645–71.
20. Saji, N.H., Goswami, B.N., Vinayachandran, P.N., Yamagata, T. 1999 A dipole mode in the tropical Indian Ocean. Nature, 401, 360–363.
21. Shetty, S., Umesh, P., Shetty, A., 2022. Dependability of rainfall to topography and micro-climate: an observation using geographically weighted regression. Theor Appl Climatol 147, 217–237. https://doi.org/10.1007/s00704-021-03811-w
22. Singh, P and Kumar N. 1997. Effect of orography on precipitation in the western Himalayan region. J. Hydrol., 199, 183–206.
23. Trenberth K.E and Hoar T.J. 1996. The 1990–1995 El Nino Southern Oscillation Event: Longest on Record. Geophys. Res. Lett., 23, 57–60.
24. Trenberth K.E and Shea D. 1987. On the evolution of the Southern Oscillation. Mon. Wea. Rev., 115, 3078–30.
25. Ubilava, D., Abdolrahimi, M., 2019. The El Niño impact on maize yields is amplified in lower income teleconnected countries. Environ. Res. Lett. 14, 054008. https://doi.org/10.1088/1748-9326/ab0cd0
26. Zhang, L., Zhao, J., Kug, J., Geng, X., Xu, H., Luo, J., Park, J., Zhan, R. 2021. Pacific warming pattern diversity modulated by Indo-Pacific sea surface temperature gradient. Geophysical Research Letters, 48. https://doi.org/10.1029/2021GL095516
27. Zhou, W., Guan, K., Peng, B., Wang, Z., Fu, R., Li, B., Ainsworth, E., DeLucia, E., Zhao, L., Chen, Z. 2021. A generic risk assessment framework to evaluate historical and future climate-induced risk for rainfed corn and soybean yield in the U.S. Midwest. Weather and Climate Extremes, 33, 100369. https://doi.org/10.1016/J.WACE.2021.100369